Quantum Electronics **37** (6) 545 – 548 (2007) ©2007 Kvantovaya Elektronika and Turpion Ltd

LASERS

PACS numbers: 42.55.Px; 42.25.Gy
DOI: 10.1070/QE2007v037n06ABEH013442

Refractive indices of solid AlGaInAs solutions

A.V. Ivanov, V.D. Kurnosov, K.V. Kurnosov, A.A. Marmalyuk,
V.I. Romantsevich, Yu.L. Ryaboshtan, R.V. Chernov

***Abstract*. The dispersion relation for refractive indices of solid AlGaInAs solutions is obtained. By using this relation, the theory is shown to be in good agreement with experimental refractive indices and the angular divergence of radiation of semiconductor lasers emitting at 1.3 and 1.55 μm.**

Keywords: *semiconductor laser, refractive index, angular radiation divergence.*

1. Introduction

The use of the AlGaInAs/InP heterostructure instead of InGaAsP/InP provided the extension of the operating temperature range of 1.3-μm and 1.55-μm semiconductor lasers up to 150 – 170 °C, reduced the threshold current [1, 2], and ensured a high reliability of the lasers without the use of microcoolers [3].

The parameters of AlGaInAs/InP heterostructure lasers were studied in papers [4 – 9]. However, the values of refractive indices reported in different papers and used in calculations of laser parameters differ from each other [8, 9] [see below curves (*2*) and (*3*) in Fig. 4]. Attempts to compare the calculated and experimental dependences of the angular divergence of laser radiation by using these data have demonstrated the discrepancy between the theory and experiment.

In this paper, we present the dispersion relation for the refractive index, which well describes experiments on the angular divergence of the 1.3-μm and 1.55-μm lasers.

2. Theory

The real [$\varepsilon_1(\omega)$] and imaginary [$\varepsilon_2(\omega)$] parts of the relative complex dielectric constant [or the real (n) and imaginary (χ) parts of the complex refractive index] satisfy the fundamental Kramers – Kronig relation [10, 11]

$$\varepsilon_1(\omega) = n^2(\omega) - \chi^2(\omega) =$$

$$= 1 + \frac{2}{\pi}\left[\text{V.p.}\int_0^\infty \frac{\omega'\varepsilon_2(\omega)}{(\omega')^2 - \omega^2}\mathrm{d}\omega'\right], \quad (1)$$

where V.p. is the Cauchy principal value of the integral.

The general shape of the fundamental absorption spectrum $\varepsilon_2(\hbar\omega)$ for most of the semiconductors is well known. The dashed curve in Fig. 1a shows the spectrum obtained in [10]. The corresponding band diagram is presented in Fig. 1b, where the vertical arrows indicate interband optical transitions forming the peculiarities of the spectrum $\varepsilon_2(\hbar\omega)$ for $\hbar\omega = E_0$, E_1 and E_2. Different variants of model representations of $\varepsilon_2(\hbar\omega)$ used for the description of the edge dispersion $n(\hbar\omega)$ are presented in Fig. 1 in paper [10].

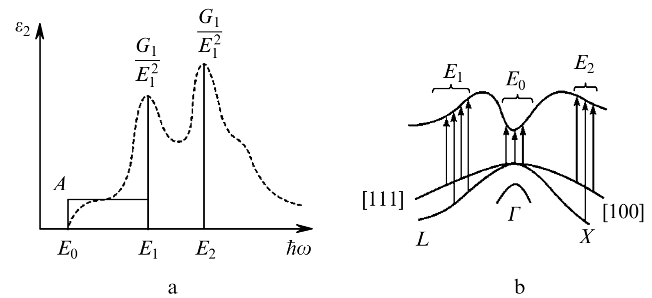

Figure 1. Model representation (solid lines) and general shape (dashed curve) of the fundamental absorption spectrum $\varepsilon_2(\hbar\omega)$ of a semiconductor (a) and its energy band diagram (b). The vertical arrows show direct transitions forming the characteristic features of the spectrum $\varepsilon_2(\hbar\omega)$; Γ, L and X are the minimal energies at the Brillouin zone centre and in directions [111] and [100], respectively.

In this paper, we use the model representation shown in Fig. 1a by solid straight lines. In the energy range from E_0 to E_1, the dependence $\varepsilon_2(\hbar\omega)$ is approximated by a constant A, while the characteristic maxima at energies E_1 and E_2 – by delta functions.

Taking relation (1) into account, the dispersion relation for $n(\hbar\omega)$ in the model representation in Fig. 1a can be written in the form [10]

$$n^2(\hbar\omega) = 1 + \frac{A}{\pi}\ln\left[\frac{E_1^2 - (\hbar\omega)^2}{E_0^2 - (\hbar\omega)^2}\right]$$

$$+ \frac{G_1}{E_1^2 - (\hbar\omega)^2} + \frac{G_2}{E_2^2 - (\hbar\omega)^2}. \quad (2)$$

A.V. Ivanov, V.D. Kurnosov, K.V. Kurnosov, A.A. Marmalyuk, V.I. Romantsevich, Yu.L. Ryaboshtan, R.V. Chernov M.F. Stel'makh Polyus Research & Development Institute, ul. Vvedenskogo 3, 117342 Moscow, Russia; e-mail: webeks@mail.ru

Received 2 October 2006; revision received 21 December 2006
Kvantovaya Elektronika **37** (6) 545 – 548 (2007)
Translated by M.N. Sapozhnikov

It was necessary to obtain for the $Al_xGa_yIn_{1-x-y}As/InP$ system the dependences of A, E_0, E_1, E_2, G_1, and G_2 on x and y. For the $Al_xGa_yIn_{1-x-y}As$ system with the lattice parameters matched ($\Delta a/a = 0$) with that of an InP crystal, the values of x and y are specified by the relation $x + y = 0.468 + 0.017x$ [12]. This expression can be written in the form $x + 1.017y = 0.476$. The approximate expression $x + y = 0.48$ is also often used.

The energy gap width E_0 for $Al_xGa_yIn_{1-x-y}As$ was defined by the expression [13]

$$E_0(Al_xGa_yIn_{1-x-y}As) = xE_0(AlAs) + yE_0(GaAs) + (1-x-y)E_0(InAs) - xyK_{AlGaAs} - y(1-x-y)K_{GaInAs} - x(1-x-y)K_{AlInAs}, \quad (3)$$

where K_{AlGaAs}, K_{GaInAs}, and K_{AlInAs} are the nonlinearity parameters of the corresponding ternary solid solutions.

The energy gap widths E_0 for AlAs, GaAs, and InAs are presented in Table 1 from [7]. The nonlinearity parameters were determined from the relation

$$E_0(Ga_yIn_{1-y}As) = yE_0(GaAs) + (1-y)E_0(InAs) + y(1-y)K_{GaInAs} \quad (4)$$

and similar relations. The values $E_0(Ga_{0.47}In_{0.53}As) = 0.75$ eV, $E_0(Al_{0.48}In_{0.52}As) = 1.45$ eV, and $E_0(Al_{0.3}Ga_{0.7}As) = 1.798$ eV were used. The value of E_0 for $Al_{0.3}Ga_{0.7}As$ was obtained from the data presented in [14]. The energy gap widths E_1 and E_2 for $Al_xGa_yIn_{1-x-y}As$ were determined from relations similar to (3).

Table 1. Values of parameters E_0, E_1, E_2, A, G_1, and G_2 for two-component solutions.

Material	E_0/eV	E_1/eV	E_2/eV	A	G_1/eV^2	G_2/eV^2
AlAs	2.95	3.8	5.3	1.5	25	110
GaAs	1.424	2.9	5.0	1.2	30	100
InAs	0.36	2.5	4.7	1.17	14.7	167

Table 1 presents the values of parameters E_0, E_1, E_2, A, G_1, and G_2 for two-component solutions AlAs, GaAs, and InAs used to calculate these parameters for four- and three-component solutions.

As a result, we found for $Al_xGa_yIn_{1-x-y}As$ the dependences

$$E_0(x,y) = 0.36 + 1.976x + 0.614x^2 + 0.622y + 0.442y^2 + 0.657xy, \quad (5)$$

$$E_1(x,y) = 2.5 + 0.686x + 0.614x^2 - 0.042y + 0.442y^2 + 0.657xy, \quad (6)$$

$$E_2(x,y) = 4.7 - 0.014x + 0.614x^2 - 0.142y + 0.442y^2 + 0.657xy. \quad (7)$$

The expressions for E_0, E_1, and E_2 were obtained by assuming the equality of nonlinearity coefficients for ternary solutions calculated by expressions similar to (4). The energy gap width E_1 and E_2 for AlGaInAs were calculated by using the values of E_1 and E_2 for AlAs, GaAs, and InP presented in Table 1 in [10].

Coefficients entering the expressions for $A(x,y)$ and $G_2(x,y)$, were corrected compared to data [10] to fit the experimental dependences of $n(\hbar\omega)$:

$$A(x,y) = 1.5x + 1.2y + 1.17(1-x-y), \quad (8)$$

$$G_1(x,y) = 25x + 30y + 14.7(1-x-y), \quad (9)$$

$$G_2(x,y) = 110x + 100y + 167(1-x-y). \quad (10)$$

Figure 2 presents the dependences of the refractive index n on the emission wavelength calculated by expression (2) and the corresponding experimental dependences obtained in [15]. One can see that calculations are in good agreement with experimental data.

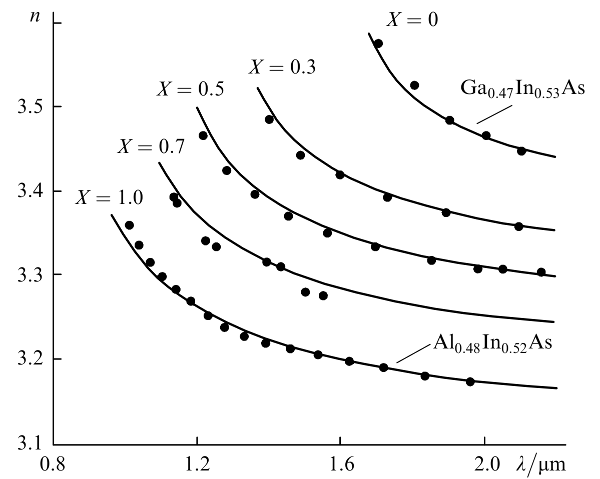

Figure 2. Wavelength dependences of the refractive index n of the $(Al_{0.48}In_{0.52}As)_X(Ga_{0.47}In_{0.53}As)_{1-X}$ heterostructure calculated by expression (2) for different values of X. Circles are experimental data [15].

Figure 3 shows the dependence of x on the energy gap width E_0 calculated from (5) for $Al_xGa_yIn_{1-x-y}As$ solutions with parameters of the InP crystal lattice [12]. One can see that the calculated dependence well agrees with experimental data.

Figure 4 shows the dependence of the refractive index n on the energy gap width E_0 calculated by expression (2) for $\lambda = 1.3$ μm for solid $Al_xGa_yIn_{1-x-y}As$ solutions matched with InP [curve (*1*)]. Curve (*2*) presents the dependence taken from [9] and curve (*3*) is drawn through three points taken from Table II from [8]. Curves (*2*) and (*3*) are also related to $\lambda = 1.3$ μm. One can see that the dependence $n(E_0)$ obtained in our paper runs virtually midway between curves (*2*) and (*3*).

To prove the validity of the found dependence $n(E_0)$, we compare the theoretical and experimental angular divergence of radiation of semiconductor lasers.

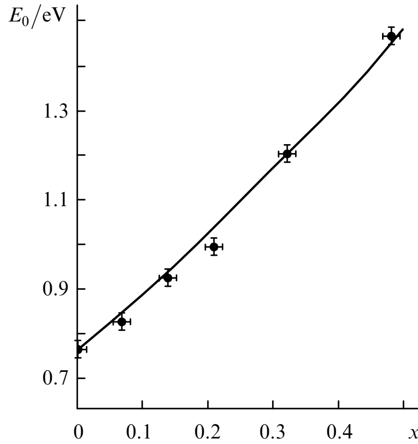

Figure 3. Dependences of the energy gap width E_0 for solid $Al_xGa_yIn_{1-x-y}As$ solutions matched with InP on x calculated from (5). Circles are experimental data [12].

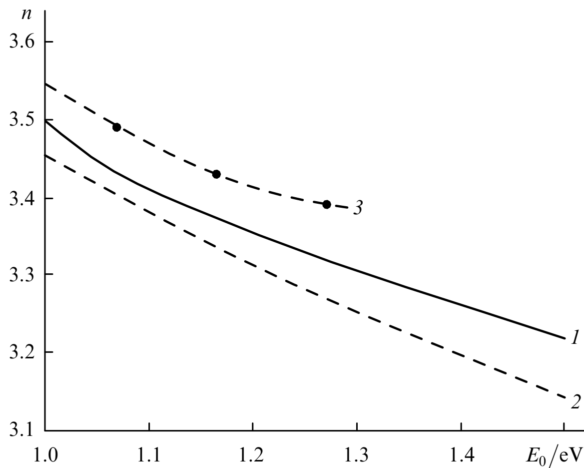

Figure 4. Dependence $n(E_0)$ for $\lambda = 1.3$ μm calculated by expression (2) for solid $Al_xGa_yIn_{1-x-y}As$ solutions matched with InP (*1*). Curve (*2*) is taken from [9], curve (*3*) is drawn through three points taken from [8].

3. Experiment

The quantum-well $Al_xGa_yIn_{1-x-y}As/InP$ heterostructures grown for experimental studies emitting at 1.3 and 1.55 μm had identically varying heights of barriers and waveguide layers. Heterostructure 1 with $x_a = 0.11$, $y_a = 0.37$, $x_b = 0.31$, $y_b = 0.17$ and heterostructure 2 with $x_a = 0.11$, $y_a = 0.37$, $x_b = 0.35$, $y_b = 0.13$ emitted at 1.3 μm; heterostructure 3 with $x_a = 0.03$, $y_a = 0.45$, $x_b = 0.2$, $y_b = 0.28$ and heterostructure 4 with $x_a = 0.03$, $y_a = 0.45$, $x_b = 0.14$, $y_b = 0.34$ emitted at 1.55 μm. The quantities x_a and y_a are related to the active region and x_b and y_b to waveguide layers. Heterostructures emitting at 1.3 and 1.55 μm had four and five quantum wells, respectively. The width of the quantum wells was 60 Å.

We fabricated quantum-well lasers from these heterostructures. The laser stripe width was 2.0–2.7 μm and the cavity length was 400 μm. Lasers were soldered on a copper heat sink, the active region up. The angular divergence of radiation was measured for each laser in the plane perpendicular to the p–n junction (in the far-field zone). In this case, the angular divergence was virtually independent of the pump current. It was shown in [16] that the angular divergence of the quantum-well laser did not change with increasing the pump current more than by a factor of four.

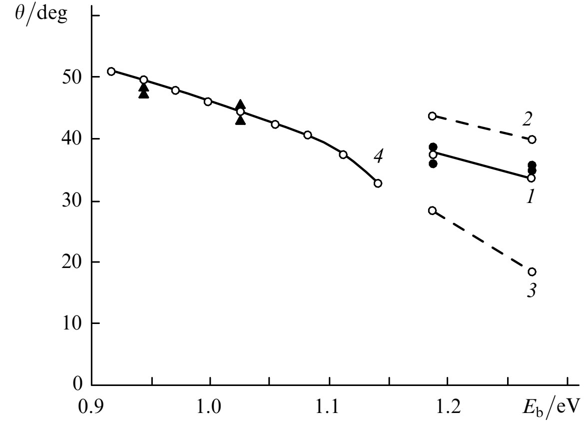

Figure 5. Dependences of the angular divergence θ of radiation on the energy gap width E_b of the waveguide layer calculated by using expression (2) (*1, 4*) and refractive indices taken from [8] (*2*) and [9] (*3*) for lasers emitting at 1.3 μm (*1–3*, ●) and 1.55 μm (*4*, ▲). Circles are experimental data.

The angular divergence calculated by using the program developed in [17] is presented in Fig. 5.

The results presented in Fig. 5 show that the angular divergences of radiation of a 1.3-μm laser calculated by using refractive indices obtained from (2) are in better agreement with experimental data than the angular divergences of radiation calculated by using refractive indices taken from papers [8] and [9]. Figure 5 also presents the angular divergence calculated by using refractive indices obtained from (2) for the 1.55-μm quantum-well laser. One can see that the calculations are in good agreement with experiment.

Thus, dispersion relation (2) for the refractive indices of solid $Al_xGa_yIn_{1-x-y}As$ solutions well describes the experimental wavelength dependences of refractive indices obtained in [15] and the angular divergence of radiation of 1.3-μm and 1.55-μm quantum-well lasers.

Acknowledgements. The authors thank A.P. Bogatov and A.E. Drakin for placing at our disposal the program for calculating the angular divergence of radiation of multilayer quantum-well lasers.

Appendix

Expression (2) has a singularity at the point E_0 where the refractive index n tends to infinity. This can be avoided taking into account the damping of the oscillator. Then, expression (2) can be written in the form

$$n^2(\hbar\omega) = 1 + \frac{A}{\pi}\ln\left\{\frac{E_1^2 - (\hbar\omega)^2}{\{[E_0^2 - (\hbar\omega)^2]^2 + (\hbar\omega E_0/k)^2\}^{1/2}}\right\} + $$

$$+ \frac{G_1}{E_1^2 - (\hbar\omega)^2} + \frac{G_2}{E_2^2 - (\hbar\omega)^2}, \quad \text{(A1)}$$

where $k = \omega_0/\gamma$; ω_0 is the resonance frequency of the oscillator; and γ is the damping parameter.

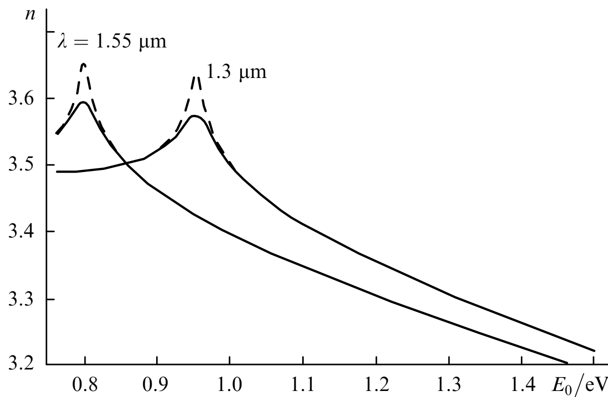

Figure 1A. Dependences of $n(E_0)$ calculated taking the damping of the oscillator into account for $\lambda = 1.3$ and 1.55 μm and $k = 30$ (solid curves) and 100 (dashed curves).

Figure 1A presents the dependences of $n(E_0)$ calculated from (A1) for $\lambda = 1.3$ and 1.55 μm and $k = 30$ [18] and 100 [19] for the $Al_xGa_yIn_{1-x-y}As$ heterostructure matched with the InP crystal $(x + y = 0.48)$.

References

1. Wang M.C., Lin W., Shi T.T., Liao H.H., Chang H.L., Su J.Y., Tu Y.K. *Proc. Conf. LEOS'95* (San Francisco, 1995) Vol. 1, p. 280.
2. Ishikawa T., Higashi T., Uchida T., Yamamoto T., Fujii T., Shoji H., Kobayashi M., Soda H. *IEEE Photon. Technol. Lett.*, **10**, 1703 (1998).
3. Vilokkinen V., Savolainen P., Sipila P. *Electron. Lett.*, **40**, 1489 (2004).
4. Zah C.-E., Bhat R., Pathak B.N., Favire F., et. al. *IEEE J. Quantum Electron.*, **30**, 511 (1994).
5. Minch J., Park S.H., Keating T., Chuang S.L. *IEEE J. Quantum Electron.*, **35**, 771 (1999).
6. Selmic S.R., Chou T.-M., Sih J.P., Kirk J.B., et. al. *IEEE J. Sel. Top. Quantum Electron.*, **7**, 340 (2001).
7. Ishikawa T., Bowers J.E. *IEEE J. Quantum Electron.*, **30**, 562 (1994).
8. Piprek J., White J.K., SpringThorpe A.J. *IEEE J. Quantum Electron.*, **38**, 1253 (2002).
9. Kazarinov R.F., Belenky G.L. *IEEE J. Quantum Electron.*, **31**, 423 (1995).
10. Pikhtin A.N., Yas'kov A.D. *Fiz. Tekh. Poluprovodn.*, **22**, 969 (1988).
11. Pikhtin A.N., Yas'kov A.D. *Fiz. Tekh. Poluprovodn.*, **12**, 1047 (1978).
12. Olego D., Chang T.Y., Silberg E., Caridi E.A., Pinczuk A. *Appl. Phys. Lett.*, **41**, 476 (1982).
13. Li E.H. *Physica E*, **5**, 215 (2000).
14. Gasey N.C. Jr., Panise M.B. *Heterostructure Lasers* (New York: Academic Press, 1978; Moscow: Mir, 1981) Vol. 1.
15. Mondry M.J., Babic D.I., Bowers J.E., Coldren L.A. *IEEE Photon. Technol. Lett.*, **4**, 627 (1992).
16. Plisyuk S.A., Akimova I.V., Drakin A.E., Borodaenko A.V., Stratonnikov A.A., Popovichev V.V., Bogatov A.P. *Kvantovaya Elektron.*, **35**, 515 (2005) [*Quantum Electron.,* **35**, 515 (2005)].
17. Popovichev V.V., Davydova E.I., Marmalyuk A.A., et al. *Kvantovaya Elektron.*, **32**, 1099 (2002) [*Quantum Electron.,* **32**, 1099 (2002)].
18. Moss T.S., Burrell G.J., Ellis B. *Semiconductor Opto-Electronics* (London: Butterworths, 1973; Moscow: Mir, 1976).
19. Peter Y., Cardona M. *Fundamentals of Semiconductors: Physics and Material Properties* (Berlin: Springer-Verlag, 2001; Moscow: Fizmatlit, 2002).